GIS-based statistical analysis of the spatial distribution of earthquake-induced landslides in the island of Lefkada, Ionian Islands, Greece

George Papathanassiou, Sotiris Valkaniotis, Athanassios Ganas & Spyros Pavlides

Landslides
Journal of the International Consortium on Landslides

ISSN 1612-510X

Landslides
DOI 10.1007/s10346-012-0357-1

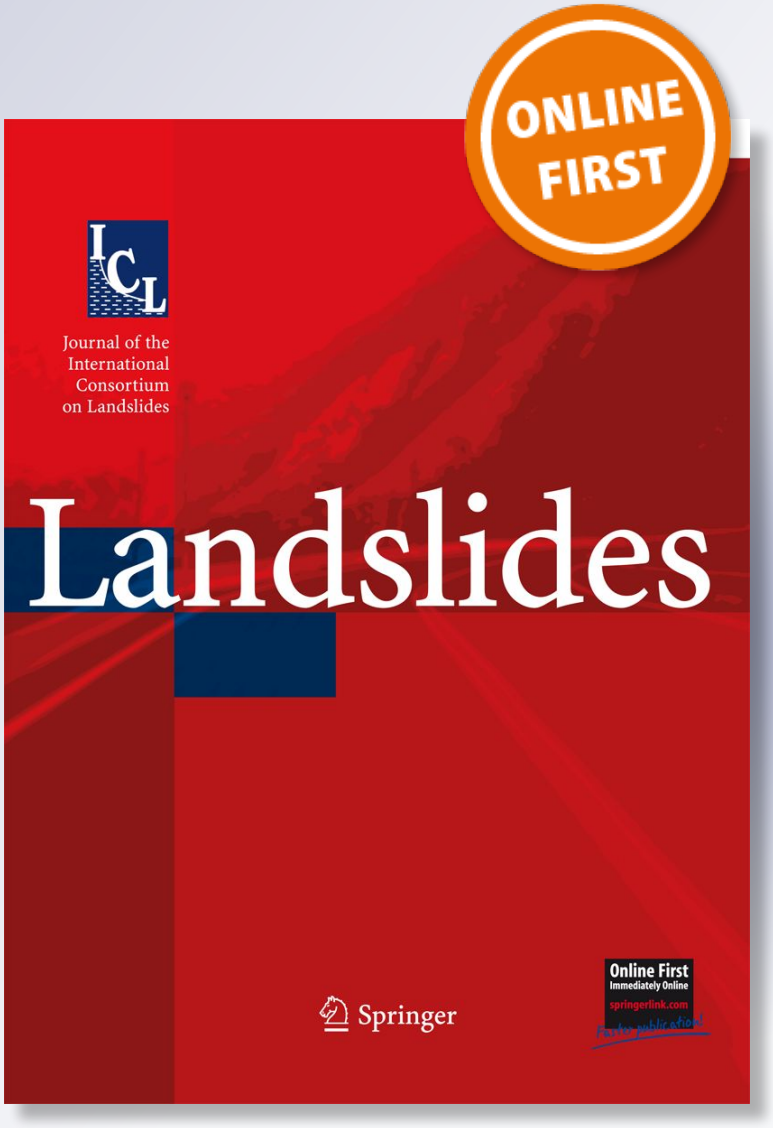

Springer

Original Paper

Landslides
DOI 10.1007/s10346-012-0357-1
Received: 26 April 2012
Accepted: 20 August 2012

George Papathanassiou · Sotiris Valkaniotis · Athanassios Ganas · Spyros Pavlides

GIS-based statistical analysis of the spatial distribution of earthquake-induced landslides in the island of Lefkada, Ionian Islands, Greece

Abstract This is the first landslide inventory map in the island of Lefkada integrating satellite imagery and reports from field surveys. In particular, satellite imagery acquired before and after the 2003 earthquake were collected and interpreted with the results of the field survey that took place 1week after this strong (Mw=6.3) event. The developed inventory map indicates that the density of landslides decreases from west to east. Furthermore, the spatial distribution of landslides was statistically analyzed in relation to the geology and topography for investigating their influence to landsliding. This was accomplished by overlaying these causal factors as thematic layers with landslide distribution data. Afterwards, weight values of each factor were calculated using the landslide index method and a landslide susceptibility map was developed. The susceptibility map indicates that the highest susceptibility class accounts for 38% of the total landslide activity, while the three highest classes that cover the 10% of the surface area, accounting for almost the 85% of the active landslides. Our model was validated by applying the approaches of success and prediction rate to the dataset of landslides that was previously divided into two groups based on temporal criteria, estimation and validation group. The outcome of the validation dataset was that the highest susceptibility class concentrates 18% of the total landslide activity. However, taking into account the frequency of landslides within the three highest susceptibility classes, more than 85%, the model is characterized as reliable for a regional assessment of earthquake-induced landslides hazard.

Keywords Rockfall · Earthquake · Lefkada · Susceptibility · Bivariate · Greece

Introduction

The population growth and the expansion of settlements and lifelines over hazardous areas are increasing the impact of natural disasters both in the developed and developing world (Alexander 1995). Casualties due to landslides are larger in the developing countries, whereas economic losses are more severe in the industrialized world. The costs of landslides range from the expense of clean-up operations and repair or replacement of structures to reduced productivity and property values. Nonetheless, landslides are considered to one of the most potentially predictable of geological hazards (Bell 1999). Nowadays, earth scientists mainly make use of geographic information system (GIS)-based techniques and remote sensing data in order to map the landslide susceptibility and hazard and evaluate the risk within an area.

Brabb (1984) define the landslide susceptibility as the likelihood of a landslide occurring in an area on the basis of local terrain conditions. The evaluation of susceptibility can be achieved using regional landslide predictive models that estimate "where" landslides are likely to occur over a given region on the basis of a set of environmental characteristics (Guzzetti et al. 1999).

In general, landslide hazard zonation techniques can be subdivided into direct and indirect methods. In direct mapping, the geomorphologist, based on his/her experience and knowledge of the terrain conditions, determines the degree of susceptibility directly. Indirect mapping uses either statistical models or deterministic models to predict landslide prone areas, based on information obtained from the interrelation between landslide conditioning factors and the landslide distribution.

GIS is very suitable for indirect landslide susceptibility mapping, in which all possible landslide-contributing terrain factors are combined with a landslide inventory map, using data integration techniques (Bonham-Carter 1994; Chung et al. 1995; van Westen et al. 2003). In particular, these factors are entered into a GIS and converted from vector-to-raster maps. After this, an overlay is made of each factor map with the landslide inventory map and the frequency statistics are calculated for the combinations of the two maps (van Westen et al. 2003).

In statistical landslide hazard analysis, the combinations of factors that have led to landslides in the past are determined statistically, and quantitative predictions are made for areas currently free of landslides but where similar conditions exist. Two different statistical approaches are used in landslide hazard analysis: bivariate and multivariate. In bivariate statistical analysis, each factor map is combined with the landslide distribution map, and weighting values based on landslide densities are calculated for each parameter class (Soeters and van Westen 1996).

This study aims to evaluate the susceptibility of landslides in the island of Lefkada by applying the bivariate statistical analysis. In order to achieve this, inventory map of landslides triggered by the 2003 earthquake was developed, and the density of landslides in relation to causal factors was computed based on the spatial distribution of the earthquake-induced landslides. Afterwards, the landslide index method (van Westen 1997) was applied and the relevant index was computed for the controlling factors. Based on this result, zones of susceptibility were delineated using the information provided by the post-earthquake inventory map (estimation group data). The flow chart shown in Fig. 1 describes the procedure that was followed in this study for the evaluation of landslide susceptibility. In addition, the model was validated using a second inventory map, which was compiled for the period before the 2003 earthquake (validation group data). The outcome of this research can be used as a basic layer for the evaluation of regional landslide hazard in the island of Lefkada.

Study area

The island of Lefkada has a rich history of strong earthquakes, being part of the high-seismicity Ionian Sea area, and consequently, earthquakes are considered the main triggering factor of landslides. Detailed reports exist in seismic catalogs and archives describing the occurrence of landslides and delineating the

Published online: 01 September 2012

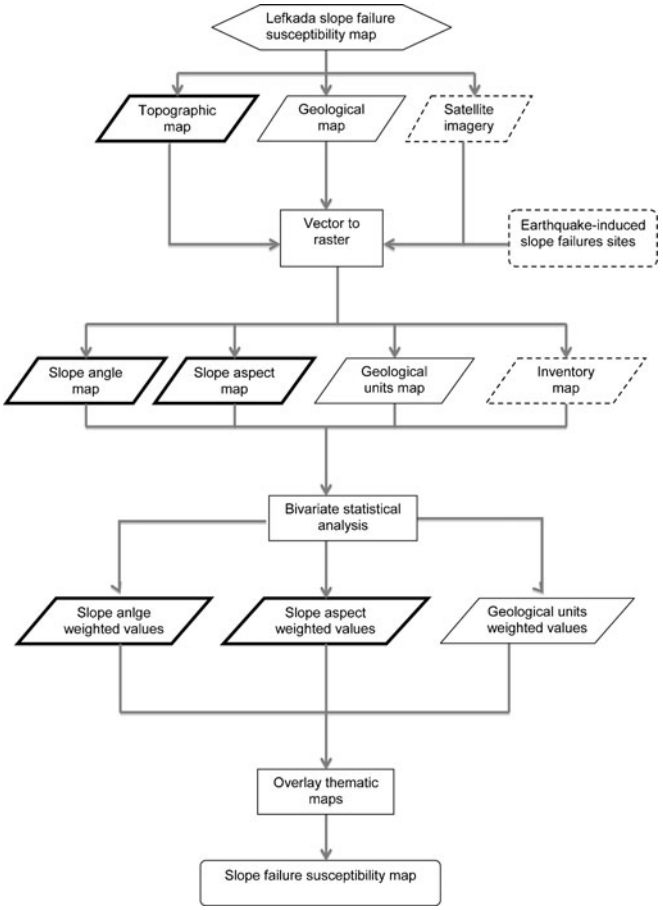

Fig. 1 Flow chart of landslide susceptibility analyses conducted in this study

western part of the island as a high-susceptibility zone. In particular, 21 earthquakes with magnitude M >5.3 occurred during the instrumental period of seismicity, from 1911 to 2011, and triggered five landslide events (Papathanassiou et al. 2011).

This conclusion is in agreement with the landslides triggered by the 14 August 2003 earthquake. In particular, the event induced characteristic rock falls, with diameters up to 4 m, observed along the 6-km-long road of Tsoukalades-Agios Nikitas, which is very close to the epicenter, and are accompanied by gravel, small rock, and soil slides (Fig. 2a). In this region, the rock falls follow the trace of a 300-m-high morphological scarp and especially a 10–40-m-high artificial slope (Fig. 2b). In most cases, rock falls are directly associated with pre-existing tectonic discontinuities and steep slopes within sedimentary rocks (Papathanassiou et al. 2005). At the center of the island, Karya village (Fig. 2a), a landslide is clearly associated to the pre-existing faults and fractures. Although many slope failure flows were observed, only few of them can be considered as typical landslides, like those along the road to Kalamitsi and Agios Petros villages (Fig. 2a).

The main active tectonic structure is the dextral strike-slip Kefalonia-Lefkada Transform fault (KLTF), last ruptured during the Mw 6.3 2003 event (Papadopoulos et al. 2003). The KLTF fault is situated just offshore the western coast of the island (Kokinou et al. 2006). The steep morphology of this coastline is due to the offshore KLTF and its onshore parallel fault, the Athani fault (Rondoyanni et al. 2007, 2012). Recent (Holocene) activity and seismic behavior of the other neotectonic faults is unknown due to lack of research (Rondoyanni et al. 2007). Recent GPS data show onshore shortening at a rate of 2–3 mm/year (Ganas et al. 2012) with velocities decreasing from north to south.

The geology of the Lefkada island, which has been studied in detail by Bornovas (1964) comprises (1) a carbonate sequence of the Ionian zone, (2) limestone of Paxos (Apulia) zone restricted in the SW peninsula of the island, (3) few outcrops of ionian flysch (turbidites), and Miocene marls–sandstones mainly in the northern part of the island (Cushing 1985; Rondoyanni-Tsiambaou 1997). A detailed map of geology (IGME 1963), is shown in Fig. 2c, where Pleistocene and especially Holocene coastal deposits (al-al.c, be-bc, and dl.l) are extended in the northern edge of Lefkada, where the homonym capital town is founded, in the valley of Vassiliki and in the coast of Nydri. Furthermore, the Ionian zone formations consist of flysch (Fi), Paleocene limestones (e-ol), limestones (K8k, j9k8, Ar-j5-8sh, and T4k, tb-tr), limestones of Pantokratora (T5-J3), dolomite (T5d); and the Paxos zone geological units consists of marls (Pm), evaporites (G), limestone (K6-8, J13k5-Jsd-Jsh), and Miocene sandstones (M-Mc-Mmk).

Developing the landslide inventory map

The compilation of an inventory map is one of the most important steps towards the development of susceptibility map and the evaluation of landslide hazard. According to Soeters and van Westen (1996), a reliable landslide inventory, defining the type and activity of all landslides as well as their spatial distribution, is essential before any analysis of the occurrence of landslides, and their relationship to the environmental conditions is undertaken.

The quality and reliability of the different analyses obtained from a landslide inventory depend largely on the quality and completeness of the original landslide map (Guzzetti et al. 1999). According to Harp et al. (2011), an inventory map is characterized as comprehensive in terms of (1) covering the entire area affected by landslides; (2) including all landslides down to a size of 1–5 m in length since it is necessary to ensure that the inventory is as complete as possible and that the landslide hazard analysis is statistically robust; and (3) depicting landslides as polygons rather than dots, representing the entire landslide, or as two or more polygons that define the landslide source and the landslide deposit.

The development of an inventory map should be based on historical information on landslide events, on field survey reports that have taken place as soon as possible after the occurrence of the triggering mechanism, the interpretation of aerial photos, and the use of satellite imagery, e.g., Google Earth. Ideally, the imagery should be continuous and span the entire landslide distribution, must have a resolution that allows identification of individual landslides as small as a few meters across and cover or be able to be draped over a digital elevation model to obtain a stereo-like perspective view (Harp et al. 2011).

In our case, the triggering mechanism of the landslides is seismic shaking and particularly, the 2003 earthquake (Mw=6.3, depth h=12 km) that occurred few kilometers offshore the island

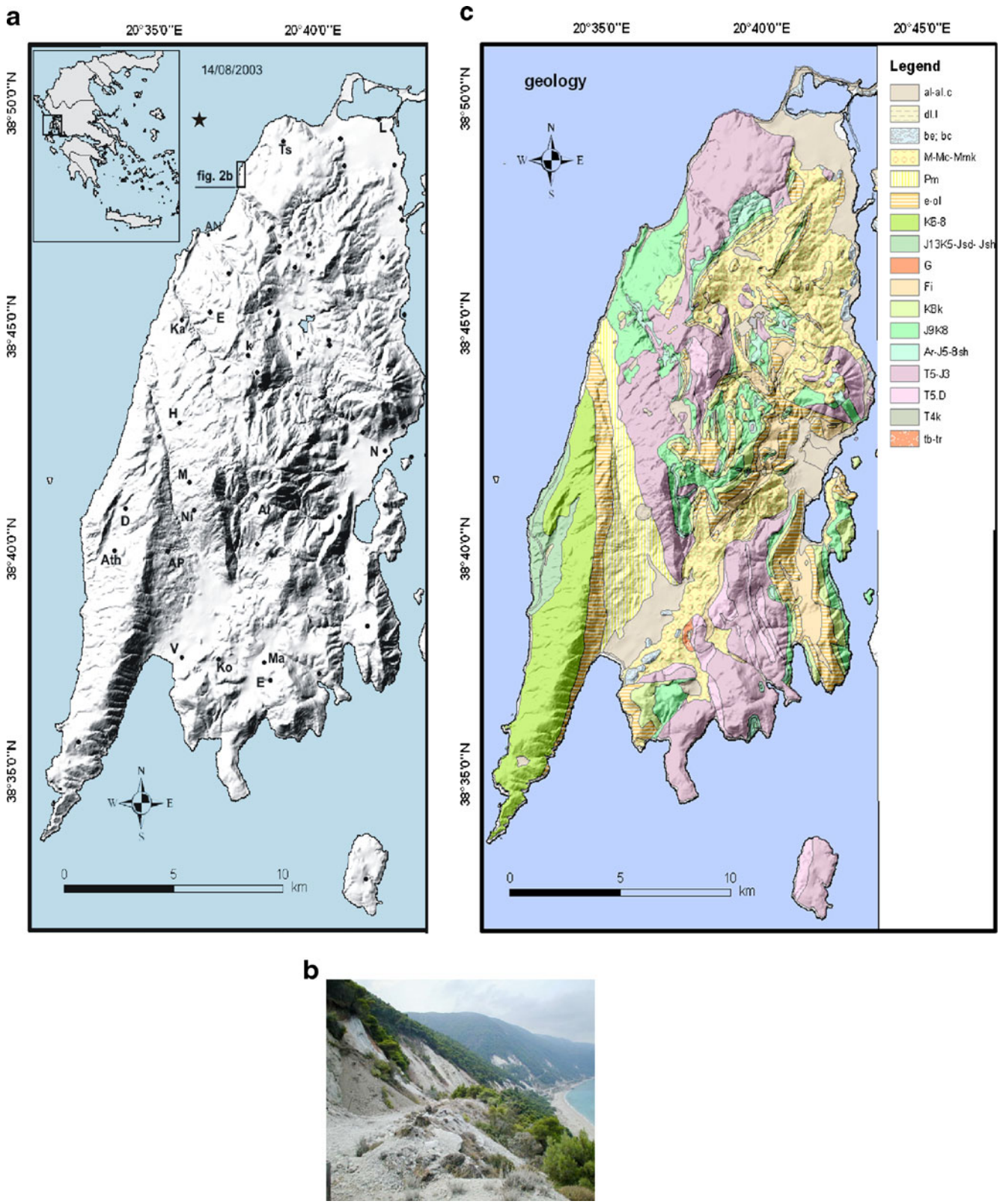

Fig. 2 **a** Map of Lefkada Island showing the epicenter (***black star***) of the 14 August 2003 earthquake. Place names referenced in the text are ***Ts*** Tsoukalades; ***AN***, Agios Nikitas; ***Ka***, Kalamitsi; ***k***, Karya; ***AP***, Agios Petros; ***L***, Lefkada; ***V***, Vassiliki; ***N***, Nydri; ***E***, Exanthia; ***H***, Hortata; ***M***, Manasi; ***Ni***, Nikolis; ***Al***, Alatron; ***D***, Dragano; ***Ath***, Athanio; ***K***, Kontaraina; ***Ma***, Marantohori; and ***E***, Evgiros. The study area is indicated by the ***black square*** in the ***left frame***. **b** Rock falls and rock slides along the road Tsoukalades–Ag Nikitas. **c** Geological map of Lefkada Island (modified from IGME 1963), where *al-al.c*, *be-bc*, *dl.l*, pleistocene and Holocene coastal deposits; *Fi*, flysch; *e-ol*, Paleocene limestones; *K8k*, *j9k8*, *Ar-j5-8sh*, and *T4k*, *tb-tr*, limestones; *T5-J3*, limestones of Pantokratora; *T5d*, dolomite; *Pm*, marls; *G*, evaporites; *K6-8*, *J13k5-Jsd-Jsh*, limestone; and *M-Mc-Mmk*, Miocene sandstones

of Lefkada; the maximum peak horizontal acceleration (PGA) was recorded at the center of Lefkada, PGA=0.42 g. The compilation of the inventory map (Fig. 3) and the evaluation of the density of landslides are based on a post-earthquake reconnaissance survey conducted few days after the event (Papathanassiou et al. 2005) and the use of cloud-free satellite imagery from Google Earth acquired on 19 December 2005. A vector-to-raster conversion was undertaken to provide raster data of landslide areas with 10 by 10-m pixels. In addition, a pre-earthquake inventory map is developed using satellite images acquired on June of 2003 (Fig. 4), 2 months before the strong earthquake. All the images that were used in our study meet the criteria proposed by Harp et al. (2011) since they covered the entire area of the island, are continuous and cloud-free, and allow the on-screen digitization of the margins of landslides.

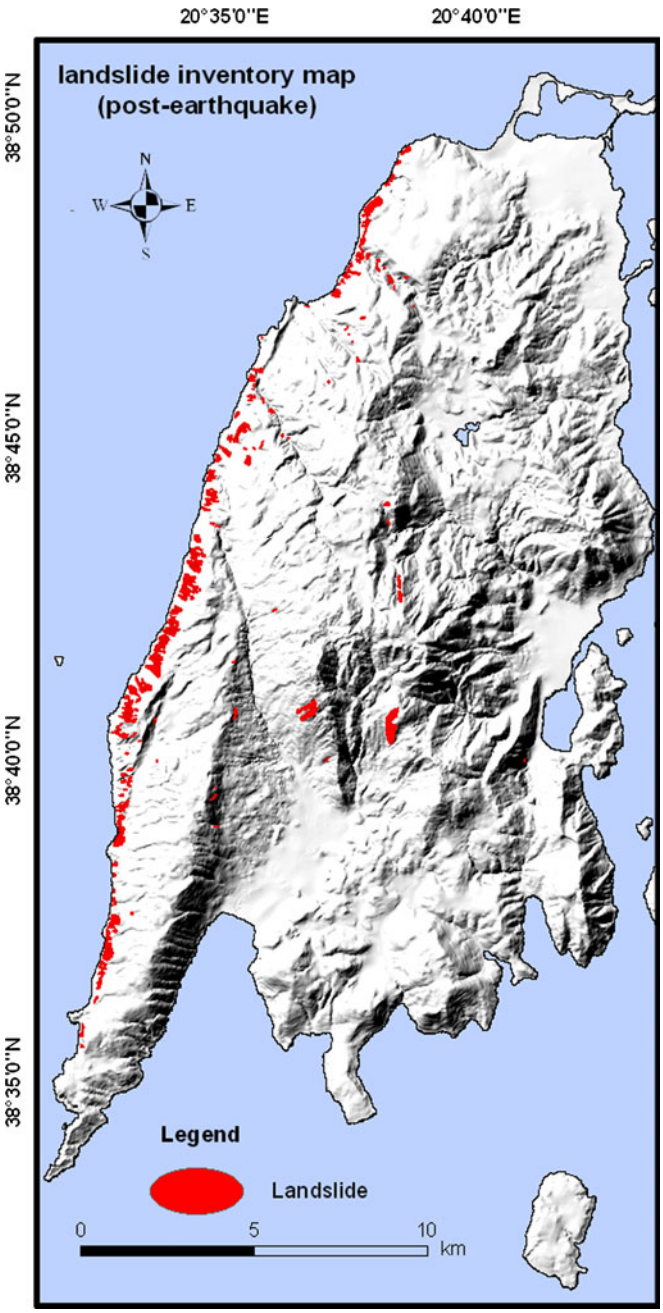

Fig. 3 Landslide inventory map compiled using post-earthquake data

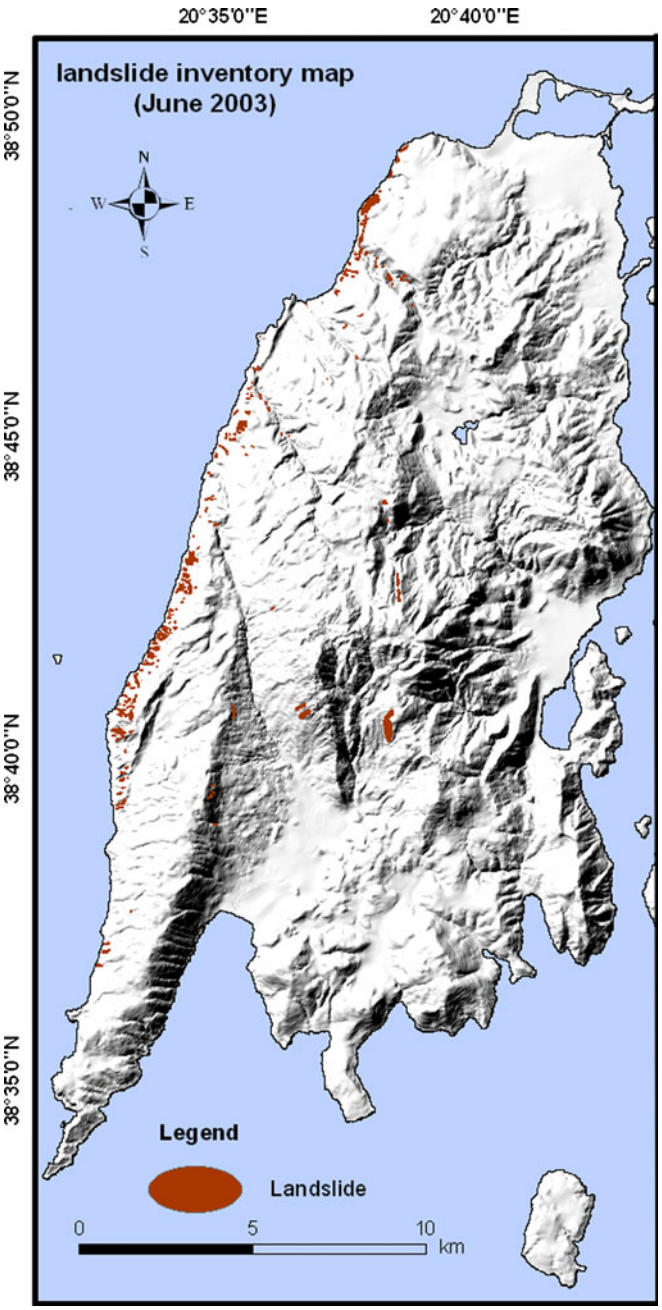

Fig. 4 Landslide inventory map compiled using data before the 2003 event

In the island of Lefkada, the dominating reported types of landslides is rock falls and slides and is frequently observed in steep slopes of sedimentary rocks. However, it was decided to use the term "landslide" in this study for defining these phenomena since it is more consistent with the existent literature. As it is shown in Fig. 3, the distribution of landslides is dense in the western part of the island, mainly in coastal zone. This is the outcome of the high level of weathering of the sedimentary rocks at the west- and northwest-facing slopes due to the precipitation and the dominating direction of wind in the island of Lefkada, and the tectonic activity in

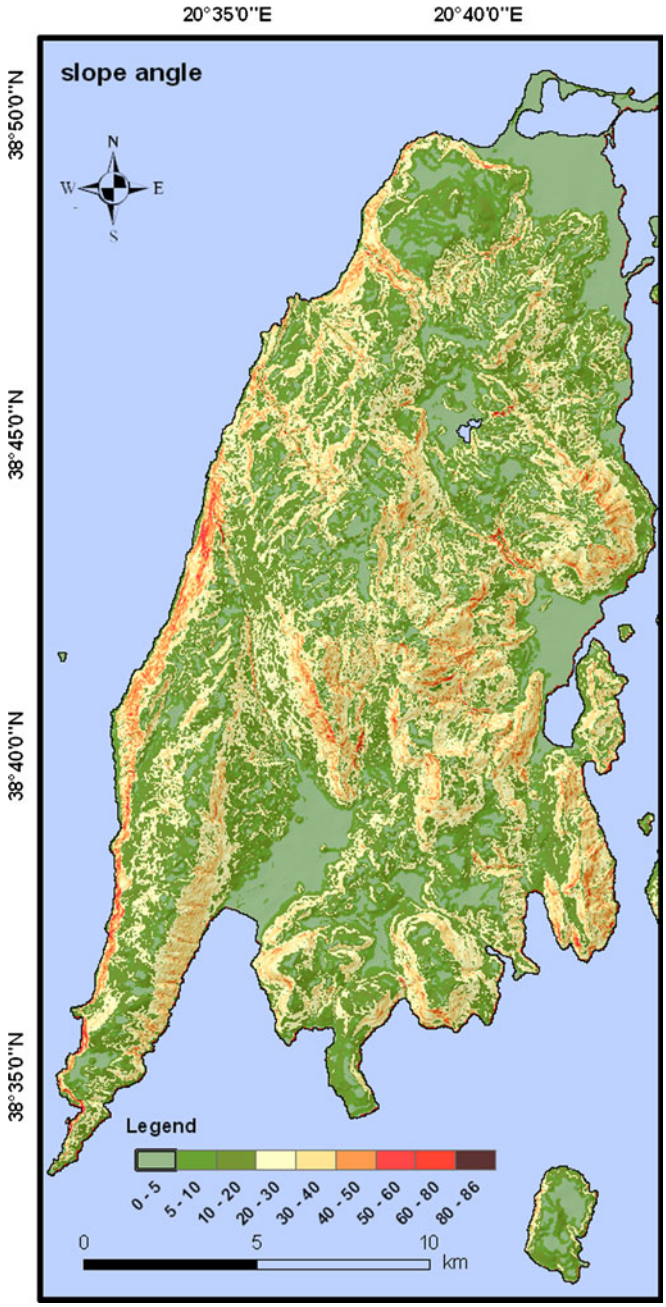

Fig. 5 Slope angle map of the Lefkada Island

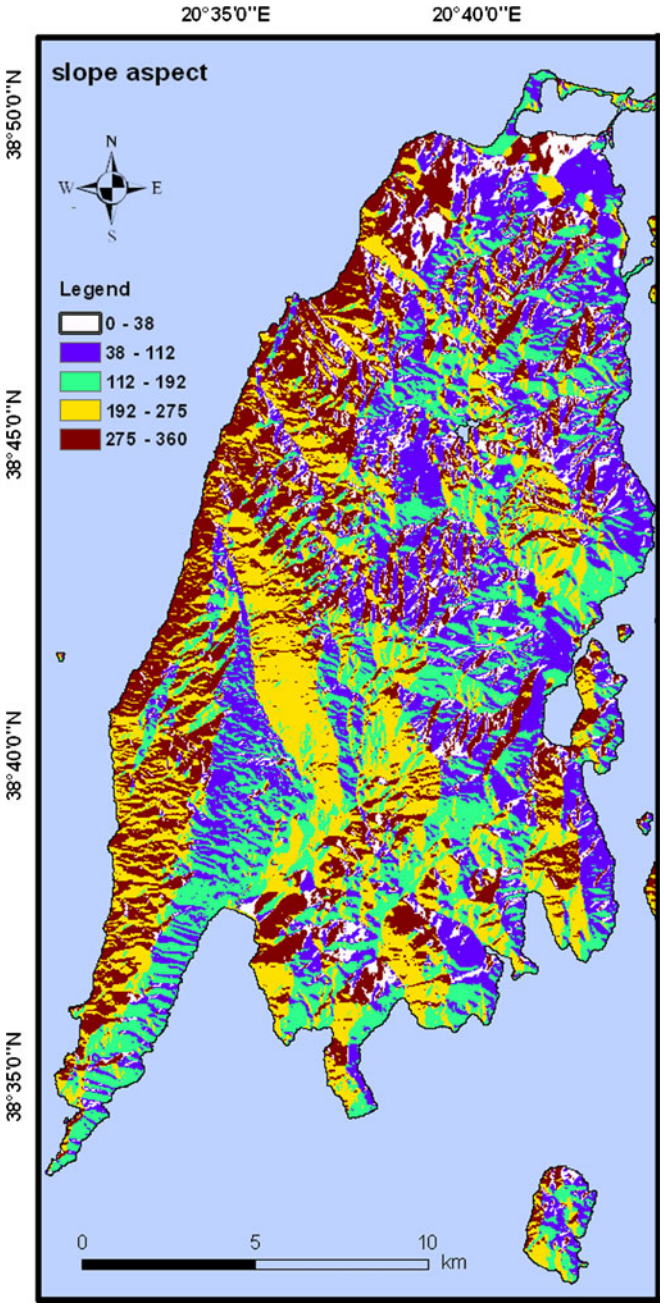

Fig. 6 Slope aspect map of the Lefkada Island

the area that highly fractured the limestones, decreasing their mechanical properties. In addition, the density decreases towards the center part of the island and is almost zero at the eastern part, mainly due to the topographic low. The surface of the study area is 301.06 km^2, while the percentage of the area affected by landslides is 1.05 % (3.17 km^2) and 0.59 % (1.8 km^2) based on data acquired after (2005) and before (2003) the triggering event, respectively.

As it is shown in Figs. 3 and 4, the two inventories are visually similar. Therefore, in order to compute their similarities, a quantitative comparison took place using the geometrical intersection and union analysis in the ArcInfo Software, respectively. The outcome provided by the analyses is that 0.85 km^2 of the landslide area (0.28 % of the total area) was common to both maps and that 4.2 km^2 of the study area (1.4 %) was classified as landslide area in both inventories maps.

Landslide density

The fundamental step for susceptibility mapping is the recognition of the factors that are responsible for landsliding. Their spatial distribution in conjunction with the mapping of areas with and without landslides is the key element for a reliable and accurate hazard assessment. These factors are defined as causals and determine all the preconditions for failure (Ayalew and Yamagishi 2005). The selection of causal factors mainly depends on the scale

Table 1 Spatial distribution of geological units and relevant slope failure density

Geological unit	Surface area %	Unit landslide density	Total landslide density	Weight factor
al-al.c	8.46	0.49	4	−0.76
Be-bc	1.32	–		
dl.l	0.06	–		
Pm	5.65	2.44	4.36	0.84
G	0.01	7.63	0.1	1.98
K6-8	9.87	2.23	21	0.75
J13k5-Jsd-Jsh	2.01	19.01	36.3	2.89
M-Mc-Mmk	16.2	0.33	5.1	−1.13
Fi	3.36	–		
e-ol	10.29	0.56	5	−0.61
K8k	5.14	0.24	1	−1.47
j9k8	10.22	0.73	7	−0.36
Ar-J5-8sh	1.35	0.41	0.5	−0.94
T5-j3	22.18	0.51	11.4	−0.7
T5d	3.22	1.28	4	0.2
T4k	0.003	–		
Tb-tr	0.52	–		

The geological units are shown on the map of Fig. 2c

of the mapping and the availability of data. According to Ayalew and Yamagishi (2005), in GIS-based studies, the selected factors should be operational, complete, non-uniform, measurable, and non-redundant.

In our study, geology, slope angle, and slope aspect are selected as causal factors. The latter was selected in order to investigate the influence of slope orientation to the occurrence and the density of landslide. The other two factors, geology and slope angle, were selected because it is well known that both are considered and most widely used as basic elements for the regional assessment of susceptibility to landslides.

Afterwards, thematic layers of geology, slope angle and aspect (Figs. 2c, 5, and 6) were developed from the Digital Elevation Model of a 10-m pixel-size grid prepared from contour lines on the 1:50,000-scale topographic map using 3D Analyst and Spatial Analyst extension of ArcInfo Software and from the geological map of the island of Lefkada (IGME 1963).

The post-2003 earthquake landslide spatial distribution, shown in Fig. 3, was correlated with each of these factors in order to develop landslide density maps, expressed as the percentage of the area affected by landslide activity. In particular, we followed the definitions proposed by Ayalew et al. (2011) in order to compute the frequency of landslide activity in the island of Lefkada in our study; the unit landslide density is the ratio between areas affected and not affected by landslides in each geological unit, and the total landslide density is the area affected by landslides in each geological unit divided by the total study area, determining the susceptibility of geological units for failure. Similar, statistical

Table 2 Spatial distribution of classes of slope aspect and relevant landslide density

Class	Aspect (deg)	Class area %	Class landslide density %	Total landslide density	Weight factor
1	0–38 northeast	8.70	0.20	2.23	−1.64
2	38–112 east	24.10	0.07	1.83	−2.76
3	112–192 southeast	21.69	0.02	0.75	−3.99
4	192–275 south west	22.51	1.10	28.32	0.05
5	275–359 northwest	23.35	2.49	66.87	0.86

Table 3 Spatial distribution of classes of slope angles and relevant landslide density

Class	Slope angle (deg)	Class area km^2	Class area %	Class landslide density (%)	Total landslide density	Weight factor
1	0–5	0.19	0.06	2.53	0.35	0.877
2	5–10	48.95	15.64	0.00	0.15	−5.549
3	10–20	41.58	13.28	0.06	0.73	−2.943
4	20–30	86.79	27.73	0.14	3.72	−2.044
5	30–40	73.89	23.61	0.55	15.20	−0.642
6	40–50	45.29	14.47	2.54	38.10	0.882
7	50–60	11.89	3.80	8.79	34.10	2.124
8	60–80	1.46	0.47	12.74	7.20	2.495
9	>80	3.225	1.03	0.38	0.39	−1.012

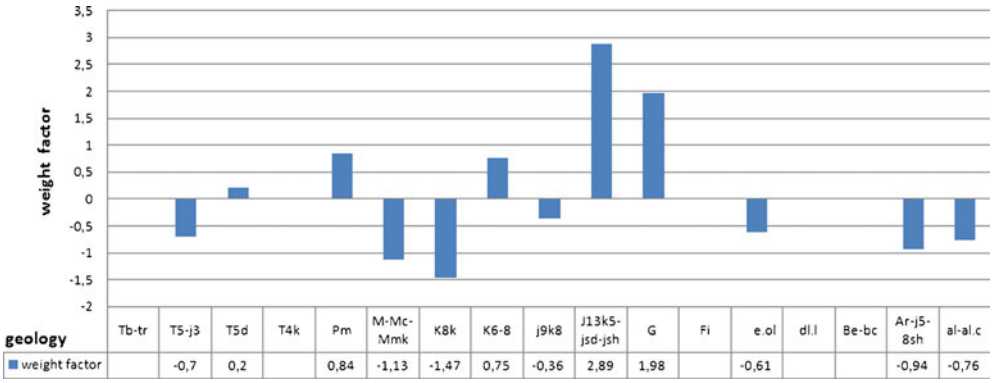

Fig. 7 Weight factor values of classes of geological units. The weight values range between 2.89 for the unit of limestones of Paxos zone and −1.47 for limestones of Ionian zone

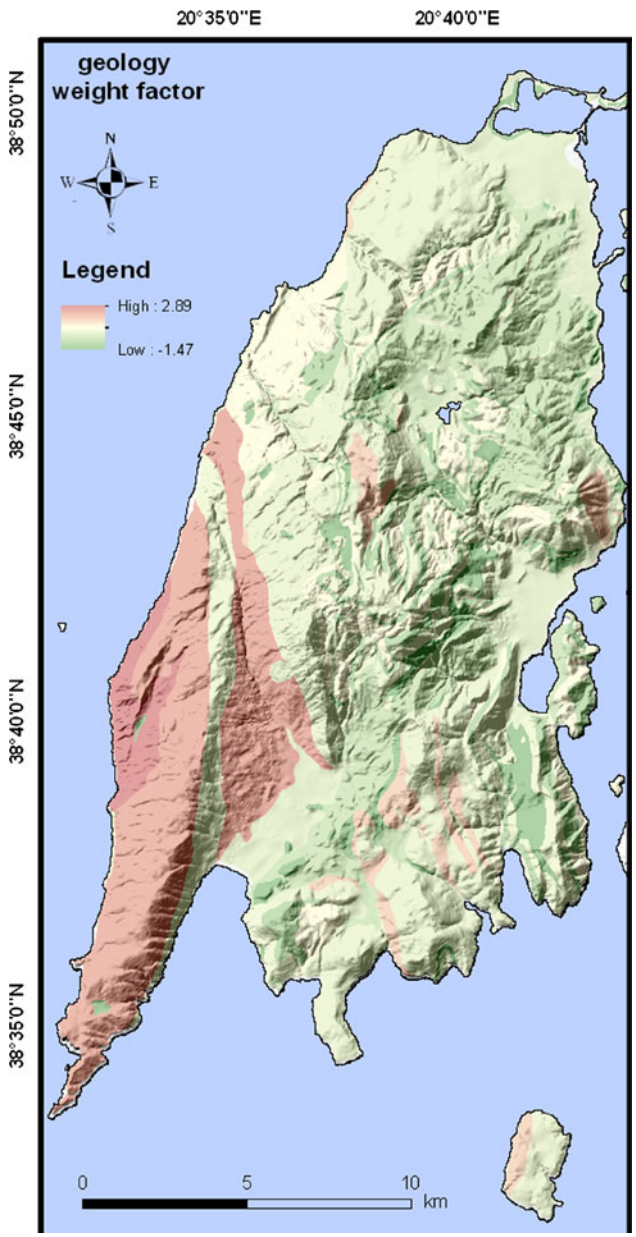

Fig. 8 Map showing the distribution of the computed weight values of the geological units

analyses was also performed for the other two factors, slope angle and slope aspect, that were taken into account in this study.

Correlation of surface geology with the spatial distribution of landslides

The correlation of spatial distribution of landslides with the geological units is listed in Table 1. It can be seen that most of the landslides are reported in areas covered by limestone (~60 %). In particular, the highest concentration of landslide activity per geological unit shows the group of units J13k5-Jsd-Jsh (19 %), where despite the fact that it covers only 2 % of the study area, the landslide activity is almost 36 % of the whole landslide activity in the island. It is followed by the unit of evaporites G that covers the 0.014 % of the study area, which was ranked with 7.63 % of the area being affected by landslides. Furthermore, the formations of T5-J3, T5d, Pm shows a landslide activity of 0.51, 1.28, and 2.44 %, respectively, which is equal to 11.4, 4, and 4.36 % of the whole landslide activity area of the island. Low percentage of landslides, reported as earth slides on coastal areas at the western part of the island, shows the geological units of al-al.c 0.49 %, while no landsliding phenomena exhibit the units of Tb-tr, T4k, Fi, dl.l, and be-bc.

Correlation of slope aspect with the spatial distribution of landslides

Slope aspect was selected in this study as one of the causal factor not because it expresses the differential weathering of slopes to wind and precipitation but due to the fact that the outcome of the inventory map clearly indicates a higher susceptibility of west-facing slopes to landsliding. Thus, it was decided to investigate the relation between slope aspect and landslides. As it is listed in Table 2, almost all the landslides are concentrated in northwest- and west-facing slopes. In particular, the frequency of landslide activity in the former slopes is equal to 66 %, while 28 % is concentrated in the latter ones. Very low values of landslide density show the slopes located at the eastern part of the island where landslide distribution does not exceed 5 % of the total activity area.

Correlation of slope angle with the spatial distribution of landslides

The dominating type of landslide activity within the study area is rock falls and slides. Thus, it is expected that steeper slopes should have higher susceptibility to landslides. This is in agreement with the statistical analysis of landslide activity in relation to the slope

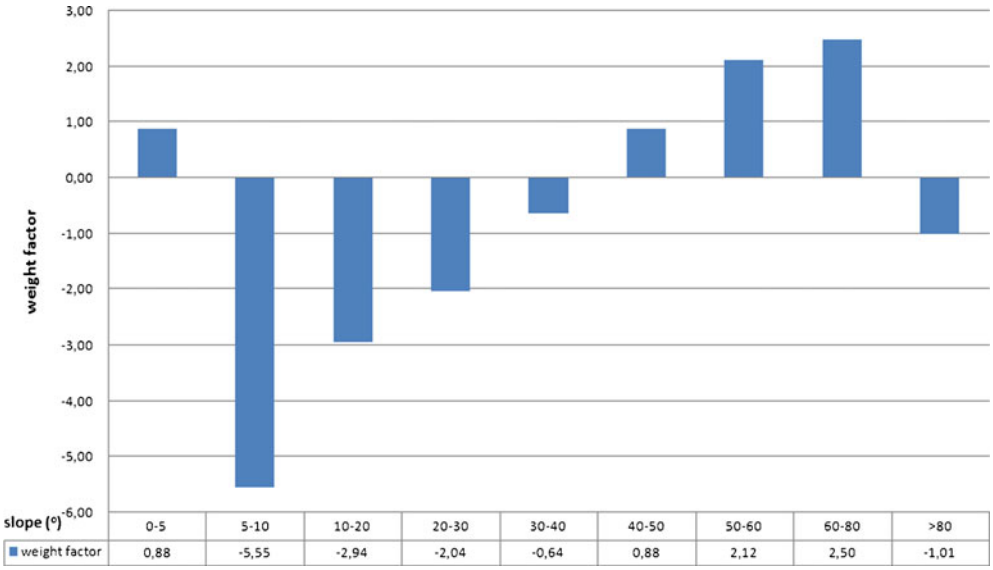

Fig. 9 Weight factor values of classes of slope angle

classes as it is listed in Table 3. In particular, landslide activity is very frequent in slope angles higher than 30°, while the highest frequency is reported in slope angle between 40 and 50°, although the fact that 50 % of the slopes within the study area is distributed from 20° to 40°. The rest of 50 % of the area is equally occupied by gentler slopes (5–10° and 10–20°) and by steeper slopes with angle between 40–50°. The resulted spatial distribution in our study is in agreement with other earthquake-induced landslides cases, such as the 1989 Loma Prieta where landslides were mainly concentrated between 30–45° (Keefer 2000) and on slopes steeper than 27° regarding the 2004 Niigata earthquakes (Wang et al. 2007).

Evaluation of landslide susceptibility using statistical (bivariate) analysis

Statistical methods are suited for assessing landslide susceptibility over complex areas especially at medium scales, ranging from 100 to 500 m³ (Cardinali et al. 2002; Clerici et al. 2006; Conforti et al. 2012). Having estimated the total and unit/class landslide density, the susceptibility to landslide was evaluated using the bivariate statistical analysis. In particular, the approach that was used in this study is the landslide index method (van Westen 1997). A weight value for a parameter class or unit is defined as the natural logarithm of the landslide density *i*, the class divided by the landslide density in the entire map. The natural logarithm is used to give negative weights when the landslide density is lower than normal and positive when it is higher than normal (van Westen 1997).

This method is based upon the following formula:

$$\mathrm{Wi} = 1n\frac{\mathrm{denClass}}{\mathrm{denMap}} = 1n\left(\frac{\frac{\mathrm{Npix(Si)}}{\mathrm{Npix(Ni)}}}{\frac{\sum \mathrm{Npix(Si)}}{\sum \mathrm{Npix(Ni)}}}\right) \quad (1)$$

where

Wi the weight given to a certain parameter class (e.g., a rock type, or a slope class).

densClass the landslide density within the parameter class.

densMap the landslide density within the entire map.

Npix(Si) number of pixels, which contain landslides, in a certain parameter class.

Npix(Ni) total number of pixels in a certain parameter class.

In Figs. 7 and 8, the weight values for the geology factor are shown. In the geology-based map, the weight values range between 2.89 for the unit of limestones of Paxos zone and −1.47 for limestones of Ionian zone. The highest weight value that was assessed based on slope angle map is equal to 2.49 for the class of slope angle 60–80° and the lowest for the class of 5–10°, equal to −5.54 (Figs. 9 and 10). The range of weight values of slope aspect map varies between 0.86 and −3.98 (Figs. 11 and 12), indicating that the significance of the factor to the triggering of landslides is not so important as the slope angle and the geology for this area. As it was analyzed in previous section, few geological units do not show any landslide activity, and consequently, the relevant unit landslide density is equal to 0.

Afterwards, the susceptibility map is compiled by overlaying the thematic layers and adding the separate weight values. The resulted values range between −9.44 and 6.24 for very low- and very high-susceptibility areas, respectively (Fig. 13). Furthermore, for visual and easy interpretation of the areas, the resulting weight value map was normalized and classified into equal areas and grouped into ten classes (Fig. 14). The area of highest susceptibility has been classified as "10", while the area of lowest susceptibility was indicated as "1".

In Figs. 14 and 15, the spatial distribution and the frequency of the landslides based on the above classification are shown. In general, the areas classified as "8", "9," and "10" cover the 10 % of the total area, while the landslide activity within these areas is equal to 85 % of the total activity. The three lowest susceptibility areas cover 37 %, and the area of landslides within these zones is less than 0.2 % of the total activity. In particular, the area classified as "10," indicating highest susceptibility, covers the 1.65 % of the total study area, while the landslide activity is 38.36 % of the total

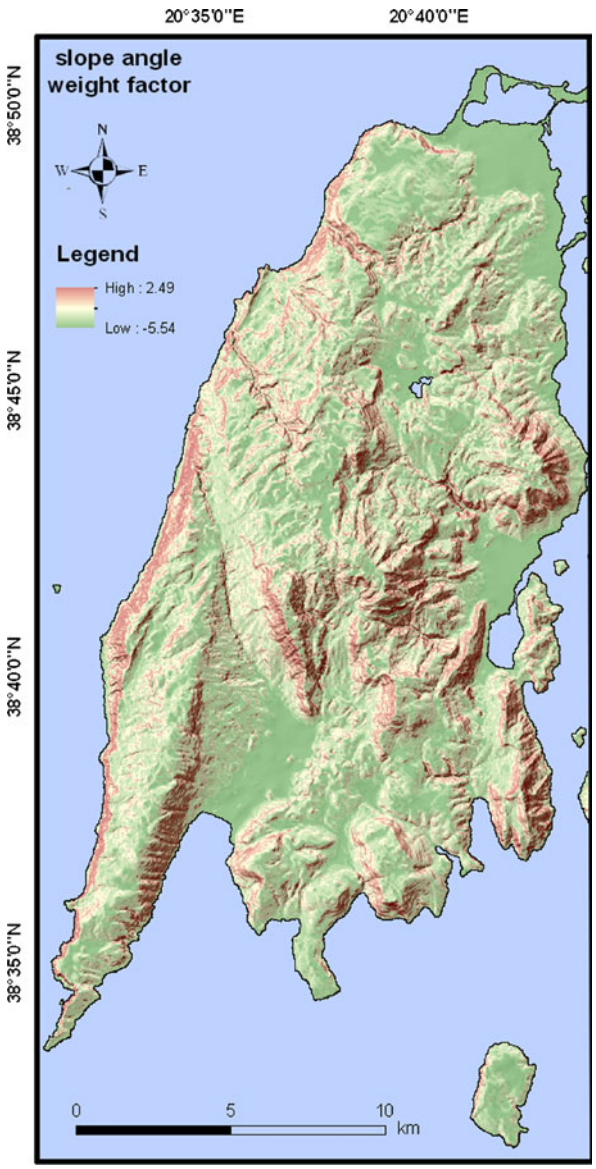

Fig. 10 Map showing the distribution of the computed weight values of the slope angle classes. The highest weight value that was assessed based on slope angle map is equal to 2.49 for the class of slope angle 60–80° and the lowest for the class of 5–10°, equal to −5.54

activity. The lowest susceptibility area, classified as "1," covers the 7.71 % of the study area and concentrates the 0.01 % of the total landslide area.

In addition, a preliminary correlation of the spatial distribution of the susceptibility classes with the local road network and the location of the settlements in the island has been attempted by overlaying the relevant layers (Fig. 16). In this figure, the susceptibility classes from "1" to "7" have been grouped within one class, so the correlation among the three highest susceptibility classes "8", "9," and "10" with the road network and the settlements could be clearly presented. The outcome provided by this correlation is that 40.1 km of the road network are located in the area classified as "8" and 17 km and 600 m in the areas "9" and "10", respectively. Taking into account that the total length of the road network is 778 km, the class "8" includes 5.16 %, class "9" includes 2.17 %, and the class of highest susceptibility "10," only 0.77 % of the total network. Regarding the location of settlements and the relevant susceptibility, it is concluded that the village of Athanio is shown with the highest susceptibility to slope instabilities, class "9," since the majority of the houses is located within this zone. In addition, part of the villages of Kalamitisi, Agios Petros, and Dragano are also situated within the class "9"; however, the percentage of the constructed houses within this class is significantly lower in comparison to the village of Athanio. Furthermore, parts of the villages of Exanthia, Hortata, Manasi, Nikolis, Alatron, Kontaraina, Marantohori, and Evgiros are situated within the susceptibility class "8". In Table 4, the villages that are situated within the three highest susceptibility classes are listed, and Fig. 2a shows their location.

Validation of the outcome

In order to evaluate the reliability of the model, the approach of success rate and prediction rate is applied for evaluating the model performance (Dietrich et al. 1995; Chung and Fabbri 2003; Neuhäuser et al. 2011). In particular, a time partition of past landslides was realized, splitting the dataset into two groups, estimation and validation groups, respectively. In our study, the data provided by the inventory map of 2005 was classified in the former group and the data before 2003 in the latter one.

The success rate assesses how many landslide sites are successfully captured by the susceptibility map, while the prediction rate calculates the percentage of the independent landslides captured with the susceptibility map of the estimation dataset (Neuhäuser et al. 2011). In particular, the success rate is calculated by ordering the

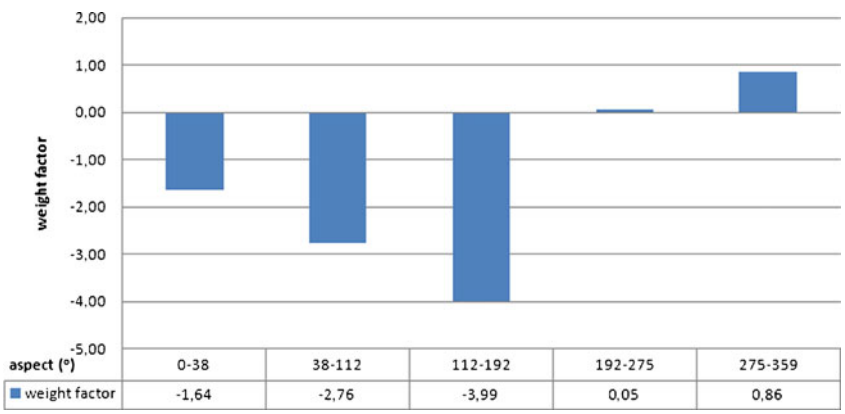

Fig. 11 Weight factor values of classes of slope aspect

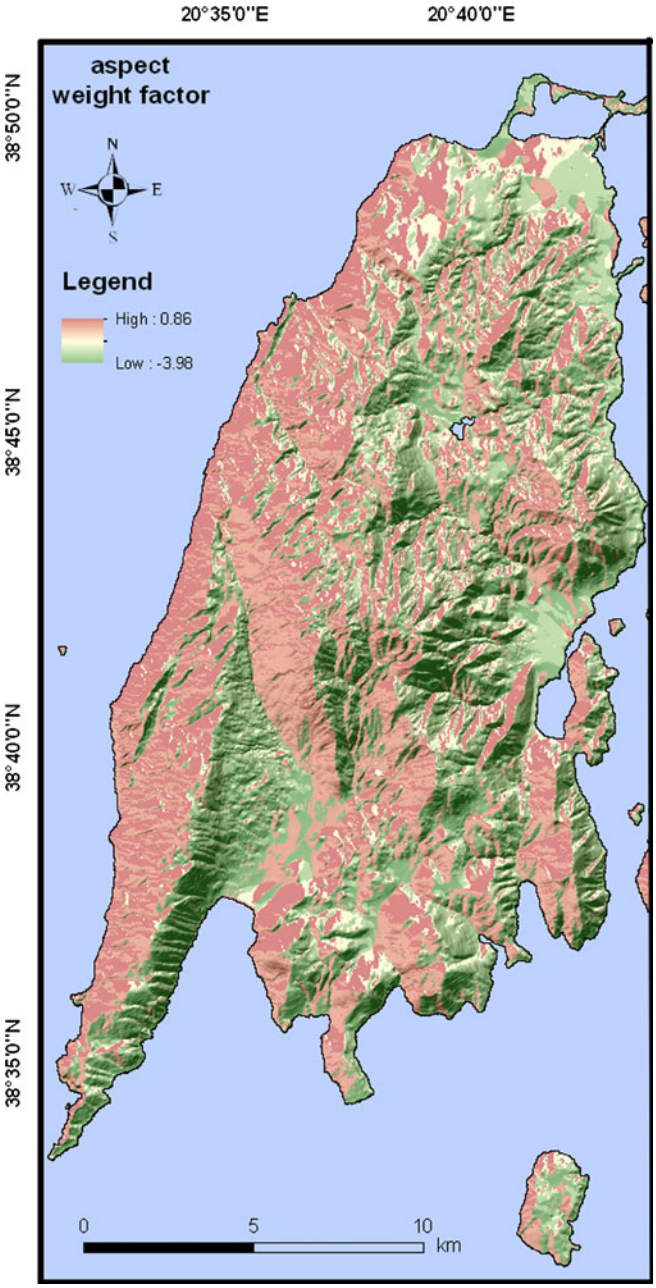

Fig. 12 Map showing the distribution of the computed weight values of the slope aspect classes. The range of the values of slope aspect map varies between 0.86 and −3.98

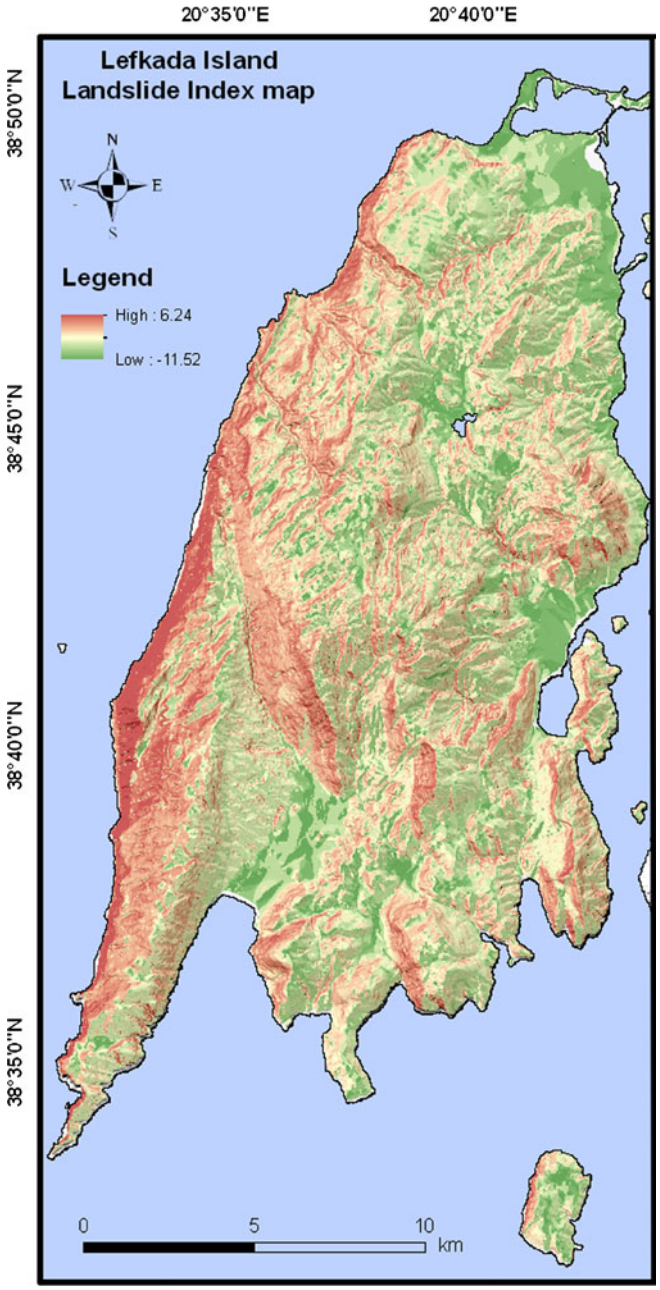

Fig. 13 Landslide Index map of Lefkada Island. The resulted values range between −9.44 and 6.24 for very low and very high susceptibility areas, respectively

pixels of a susceptibility map in number of classes, from high to low values, based on the frequency information from the histogram. Afterwards, an overlay is made with the landslide inventory map, and the joint frequency is calculated. The success rate indicates how much percentage of all landslides occurs in the classes with the highest values of the different combination maps (van Westen et al. 2003). The prediction rate curve represents the cumulative percentage of the validation set area, with respect to the cumulative percentage of the study area, ordered according to the decreasing susceptibility ranking (Conforti et al. 2012).

The inventory map produced by the mapping of landslides before the 2003 event (Fig. 4) was compared with the classification of areas, classes "10" to "1," that were developed using the estimation dataset (post-2003 earthquake inventory). The outcome provided by the overlay of these two maps is shown in Fig. 17 where the distribution of the landslide activity is correlated to the classified areas. From this overlay, it is shown that most of the landslide activity (39 %) is concentrated within the area classified as "8", while the highest landslide activity per class is shown in class "9." In addition, the landslide activity within the three highest susceptibility areas is equal to 87 % of the total activity, while the relevant activity within the three lowest susceptibility areas is less than 0.5 %.

In Fig. 18, both the success and prediction rate curves that were calculated using the estimation and validation dataset, respectively,

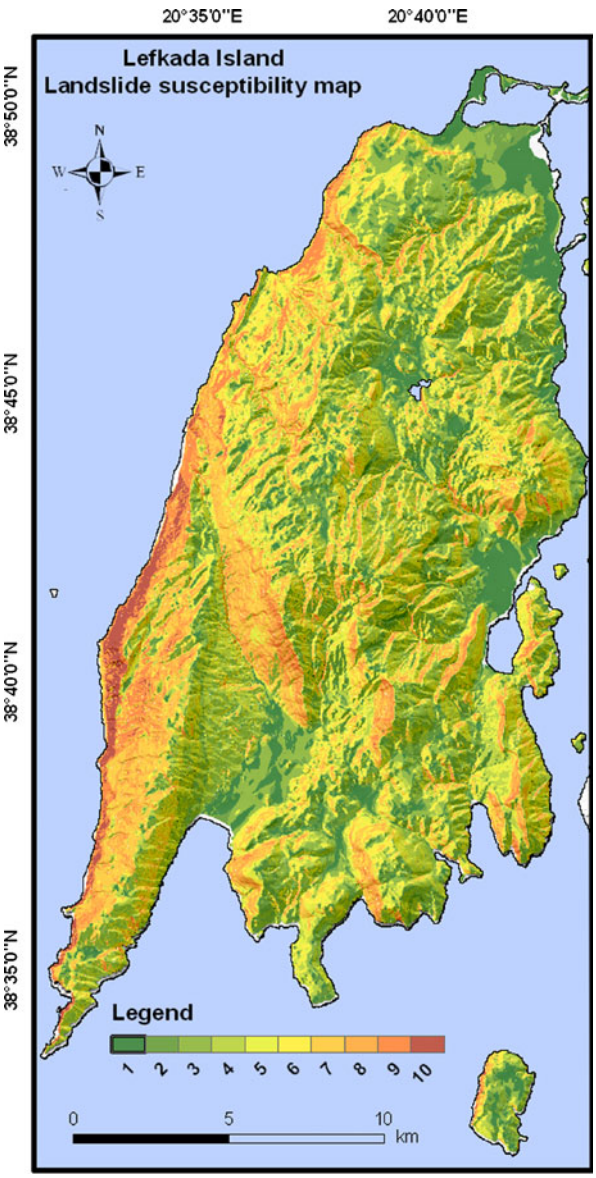

Fig. 14 Lefkada Island landslide susceptibility map. The areas classified as "8", "9," and "10" cover the 10 % of the total area, while the landslide activity within these areas is equal to 85 % of the total activity

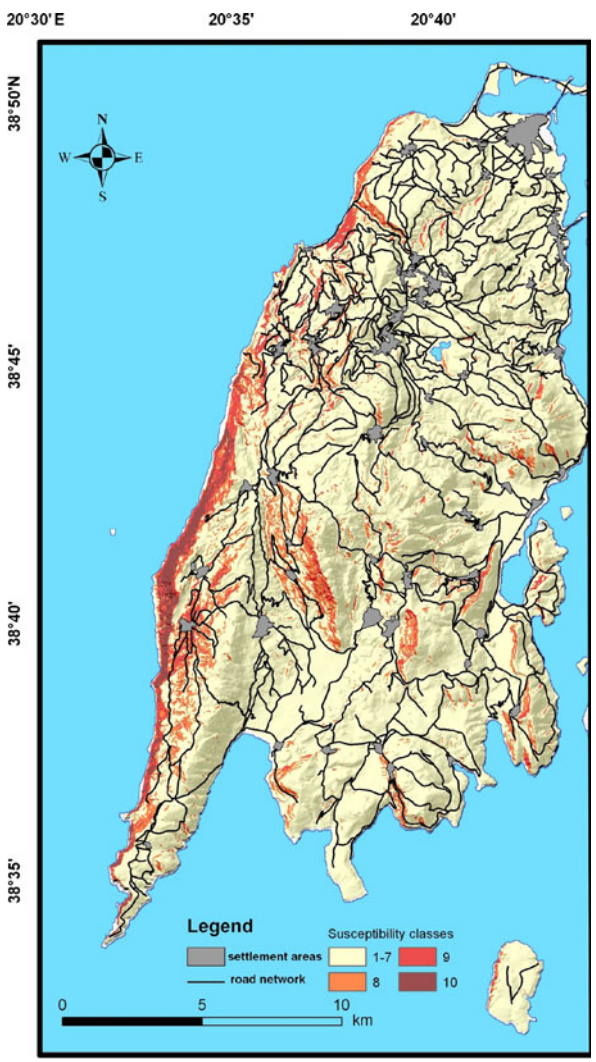

Fig. 16 Map showing the road network and the settlement areas in the Lefkada Island in relation to the susceptibility classes. The outcome provided by this study is that 40.1 km of the road network are located in the area classified as "8" and 17 km and 600 m in the areas "9" and "10," respectively

are listed. In order to examine the reliability of the model, Conforti et al. (2012) concluded that the greater the slope of the first part of the

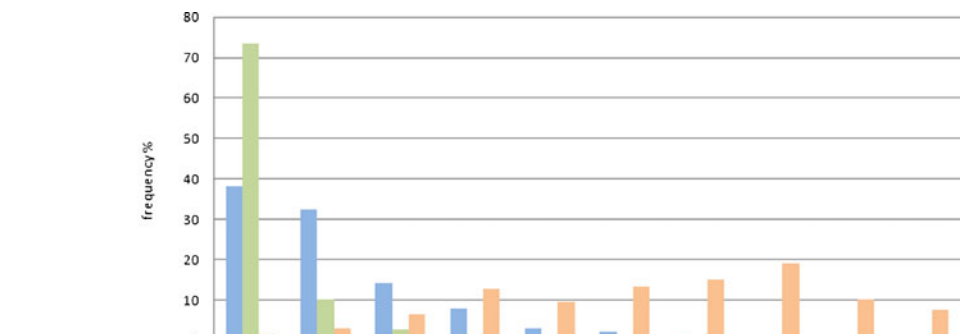

susceptibility class	10	9	8	7	6	5	4	3	2	1
frequency landslides	38,26	32,44	14,29	7,95	3,09	2,18	0,62	0,14	0,02	0,01
frequency landslides per class	73,32	10,23	2,74	0,63	0,32	0,16	0,021	0,006	0,002	0,0015
frequency class	1,65	3,02	6,65	13,04	9,72	13,5	15,14	19,14	10,32	7,71

Fig. 15 Spatial distribution of classes of landslide susceptibility map and their correlation with the captured landslide areas

Table 4 Correlation of susceptibility class and spatial distribution of settlements

Name	Id[a]	Class
Kalamitsi	Ka	9
Exanthia	E	8
Hortata	H	8
Manasi	M	8
Nikolis	Ni	8
Alatron	Al	8
Agios Petros	AP	9
Dragano	D	9
Athanio	Ath	9
Kontaraina	Ko	8
Marantohori	Ma	8
Evgiros	E	8

The location of the settlements is shown in Fig. 2a

[a] Fig. 2a

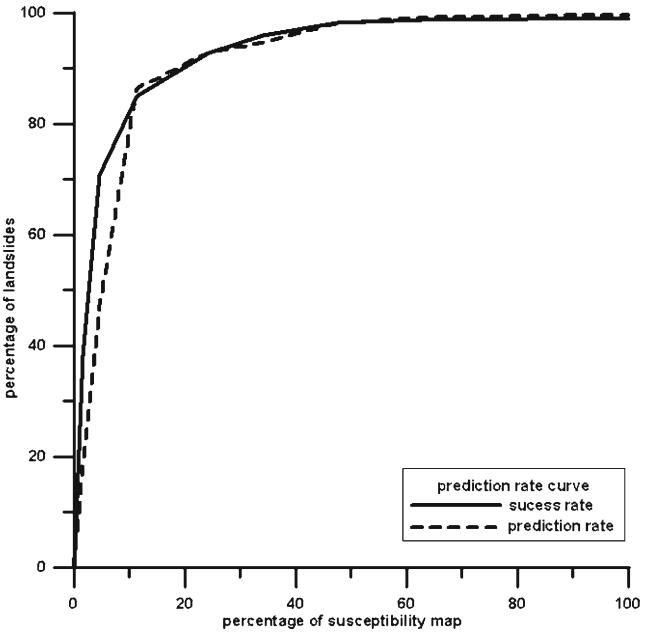

Fig. 18 Success and predicted rate curves of the susceptibility map produced for Lefkada Island. The success rate curve shows that within 10 % of the susceptibility map, more than 80 % of the landslides are included. At the same percentage of susceptibility units, the prediction rate curve shows that more than 85 % of landslides could be predicted

predicted curve and the further away from the diagonal trend, the better the predictive reliability. Following this suggestion, we can see that in our case, the high sloping of the curves in their first part indicates a good performance of the model and, thus, a good reliability of the procedure including the selection of the causal factors. In particular, the resulted success rate curve shows that within 10 % of the susceptibility map, more than 80 % of the landslides are included. At the same percentage of susceptibility units, the prediction rate curve shows that more than 85 % of landslides could be predicted. Both relations indicate that our model shows high model efficiency. In addition, 30 % of the susceptibility map captures (estimation group) and predicts (validation group) more than 90 % of landslides.

Conclusions

This study focused on investigating the influence of geology and topography on the occurrence of landslides in the island of Lefkada. In order to examine the role of these two causal factors to the generation of landslides, an inventory map of the island of Lefkada was developed for the first time based on information provided by satellite imagery and field survey reports that had taken place after the strong 2003 earthquake. The outcome of the inventory map was that landslide areas are mainly concentrated to the western part of the island and particularly to the coastal area where steep slopes are observed.

Furthermore, as it was resulted by the overlaying of the spatial distribution of landslides with the thematic layers of geology, slope aspect and slope angle, the highest frequency of landslides are related with the geological formation of limestones of Paxos zone, with west- and northwest-facing slopes and slope angle between 40–50°.

Based on this outcome, areas prone to landslides were delineated, and the relevant susceptibility in the island of Lefkada was evaluated.

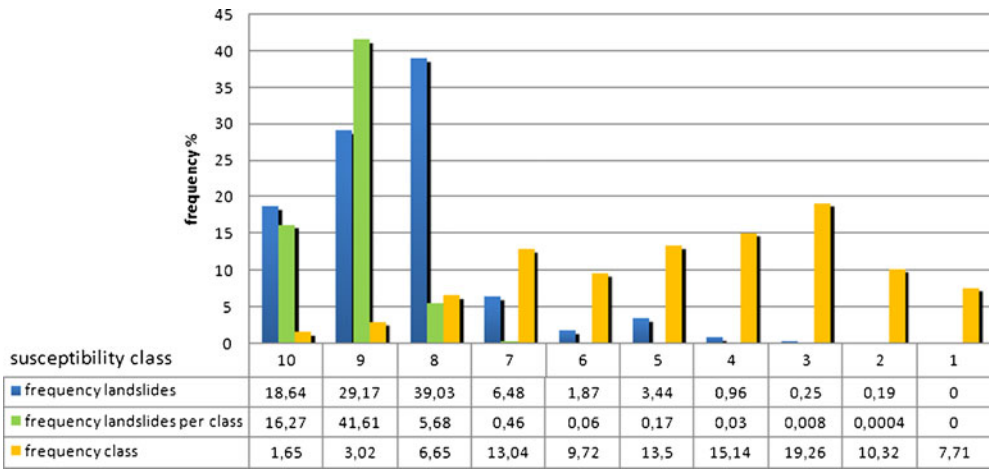

susceptibility class	10	9	8	7	6	5	4	3	2	1
frequency landslides	18,64	29,17	39,03	6,48	1,87	3,44	0,96	0,25	0,19	0
frequency landslides per class	16,27	41,61	5,68	0,46	0,06	0,17	0,03	0,008	0,0004	0
frequency class	1,65	3,02	6,65	13,04	9,72	13,5	15,14	19,26	10,32	7,71

Fig. 17 Spatial distribution of areas that are predicted as landslide activity zones

This was accomplished using the bivariate statistical analyses and in particular by applying the landslide index method. The weight values that were computed for each factor were added in order to develop a landslide susceptibility map. The resulting weight value map was normalized and classified into equal areas and grouped into 10 classes. The highest susceptibility area covers the 1.65 % of the total study area, and the landslide activity is 38.36 % of the total activity. The lowest susceptibility area covers the 7.71 % of the study area and concentrates the 0.01 % of the total landslide area. It must be taken into account that our model was based on the 2003 activation of the northern part of the KLTF fault, an area where earthquakes occurred several times the last 500 years, as it is indicated by seismic catalogs.

In order to validate the outcome of the study, we proceed to the compilation of a second inventory map using satellite imagery acquired before the 2003 event. The spatial distribution of the second inventory map was overlaid to the susceptibility map and statistically analyzed. The resulted prediction rate curve indicates that within 10 % of the susceptibility map, more than 85 % of the landslides could be predicted. In addition, 30 % of the susceptibility map predicts more than 90 % of landslides.

The resulting map provides quantitative information regarding the susceptibility to landslides and can be used by urban planners and stakeholders for reducing the risk of structures and lifelines on the island of Lefkada.

Acknowledgments

The authors of this study would like to thank the two anonymous reviewers for their critical and constructive comments which improved the quality of this manuscript. We acknowledge use of GIS data produced under the framework of projects PREVIEW and TERRAFIRMA.

References

Alexander ED (1995) A survey of the field of natural hazards and disaster studies. In: Carrara A, Guzzetti F (eds) Geographical information systems in assessing natural hazards. Kluwer Academic, Dordrecht, pp 1–19

Ayalew L, Yamagishi H (2005) The application of GIS-based logistic regression for landslide susceptibility mapping in the Kakuda-Yahiko Mountains, Central Japan. Geomorphology 65:15–31

Ayalew L, Kasahara M, Yamagishi H (2011) The spatial correlation between earthquakes and landslides in Hokkaido (Japan), a GIS-based analysis of the past and the future. Landslides 8:443–448

Bell F (1999) Geological hazards, their assessment, avoidance and mitigation. E & FN Spon, London

Bonham-Carter GF (1994) Geographic information systems for geoscientist: modeling with GIS. Pergamon, New York, pp 302–334

Bornovas J (1964) Géologie de l'île de Lefkade, Geol Geoph Res. 10

Brabb E (1984) Innovative approaches to landslide hazard and risk mapping. Proc Fourth Int Symp Landslides 1:307–323

Cardinali M, Carrara A, Guzzetti F, Reichenbach P (2002) Landslide hazard map for the Upper Tiber River basin.CNR, Gruppo Nazionale per la Difesa dalle Catastrofi Idrogeologiche, Publication n. 2116, scale 1:100,000

Chung CJF, Fabbri A (2003) Validation of spatial prediction models for landslide hazard mapping. Nat Hazard 30:451–472

Chung CJ, Fabbri A, van Westen CJ (1995) Multivariate regression analysis for landslide hazard zonation, In: Carrara A, Guzetti F (eds) Geographical information systems in assessing natural hazards. Kluwer, pp 107–133

Clerici A, Perego S, Tellini C, Vescovi P (2006) A GIS-based automated procedure for landslide susceptibility mapping by the conditional analysis method: the Baganza valley case study (Italian Northern Apennines). Environ Geol 50:941–961

Conforti M, Robustelli G, Muto F, Critelli S (2012) Application and validation of bivariate GIS-based landslide susceptibility assessment for the Vitravo river catchment (Calabria, south Italy). Nat Hazard 61:127–141

Cushing M (1985) Evoluation structurale de la marge nord-ouest hellenique dans l'ile de Lefkada et ses environs (Greece nord-occidentale), Ph.D. Thesis, Univ. de Paris-Sud (XI), Centre d'Orsay, France

Dietrich EW, Reiss R, Hsu ML, Montgomery DR (1995) A process-based model for colluvial soil depth and shallow landsliding using digital elevation data. Hydrol Process 9:383–400

Ganas A et al (2012) GPS-derived estimates of crustal deformation in the central and north Ionian Sea, Greece: 3-yr results from NOANET continuous network data. J Geodyn http://dx.doi.org/10.1016/j.jog.2012.05.010

Guzzetti F, Carrara A, Cardinali M, Reichenbach P (1999) Landslide hazard evaluation: a review of current techniques and their application in a multi-scale study, Central Italy. Geomorphology 31:181–216

Harp E, Keefer D, Sato H, Yagi H (2011) Landslide inventories: the essential part of seismic landslide hazard analyses. Eng Geol 22:9–21. doi:10.1016/j.enggeo.2010.06.013

IGME (1963) Geological map of Greece. Institute of Geological and Mineral Exploration, Greece

Keefer DK (2000) Statistical analysis of an earthquake-induced landslide distribution—the 1989 Loma Prieta California event. Eng Geol 58:213–249

Kokinou E, Papadimitriou E, Karakostas V, Kamberis E, Vallianatos E (2006) The KefaloniaTranform Zone (offshore Western Greece) with special emphasis to its prolongation towards the Ionian Abyssal plain. Mar Geophys Res 27:241–252

Neuhäuser B, Damm B, Terhorst B (2011) GIS-based assessment of landslide susceptibility on the base of the weights-of-evidence model. Landslides. doi:10.1007/s10346-011-0305-5

Papadopoulos GA, Karastathis VK, Ganas A, Pavlides SB, Fokaefs A, Orfanogiannaki K (2003) The Lefkada, Ionian Sea (Greece), shock (Mw 6.2) of 14 August 2003: evidence for the characteristic earthquake from seismicity and ground failures. Earth Planets Space 55:713–718

Papathanassiou G, Pavlides S, Ganas A (2005) The 2003 Lefkada earthquake: field observation and preliminary microzonation map based on liquefaction potential index for the town of Lefkada. Eng Geol 82:12–31

Papathanassiou G, Valkaniotis S, Pavlides Sp (2011) Evaluation of the temporal probability of earthquake-induced landslides in the island of Lefkada, Greece. Proc. 2nd World Landslide forum, Rome, Italy

Rondoyanni-Tsiambaou Th (1997) Les seismes et l'environnement géologique de l'île de Lefkade, Grèce: Passe et Future. In: Marinos P et al. (eds) Engineering Geology and the Environment. Balkema, pp 1469–1474

Rondoyanni Th, Mettos A, Paschos P, Georgiou Ch (2007) Neotectonic map of Greece, scale1:100.000, Lefkada sheet. I.G.M.E., Athens

Rondoyanni T, Sakellariou M, Baskoutas J, Christodoulou N (2012) Evaluation of active faulting and earthquake secondary effects in Lefkada Island, Ionian Sea, Greece: an overview. Nat Hazards 61(2):843–860

Soeters R, van Westen CJ (1996) Slope Instability Recognition, Analysis and Zonation. In: Turner AK, Schuster RL (eds) Landslides, investigation and mitigation, Transportation Research Board, National Research Council, Special Report 247. National Academy, Washington D.C, pp 129–177

van Westen CJ (1997) Statistical landslide hazard analysis. ILWIS 2.1 for windows application guide. ITC Publication, Enschede, pp 73–84

van Westen CJ, Rengers N, Soeters R (2003) Use of geomorphological information in indirect landslide susceptibility assessment. Nat Hazard 30:399–419

Wang HB, Sassa K, Xu WY (2007) Analysis of a spatial distribution of landslides triggered by the 2004 Chuetsu earthquakes of Niigata Prefecture, Japan. Nat Hazard 41:43–60

G. Papathanassiou (✉) · S. Valkaniotis · S. Pavlides
Department of Geology,
Aristotle University of Thessaloniki,
Thessaloniki, Greece
e-mail: gpapatha@auth.gr

A. Ganas
Institute of Geodynamics,
National Observatory of Athens,
Athens, Greece